Gait & Posture 100 (2023) 27–32

Contents lists available at ScienceDirect

Gait & Posture

journal homepage: www.elsevier.com/locate/gaitpost

Angle measurement stability and cycle counting accuracy of hours-long duration IMU based arm motion tracking with application to normal shoulder ADLs

Bryan Kirking

Enovis, 9801 Metric Blvd, Austin, TX 78758, United States

ARTICLE INFO

Keywords:
Shoulder
Inertial measurement unit
Motion
Upper limb
Cycle counting

ABSTRACT

Background: Inertial measurement units are increasing used for monitoring joint motion, but there is a need to demonstrate their suitability during hours-long continuous use, as well as a need for validated methods to count arm cycles and provide descriptions of typical cycles.

Research question: Do IMU sensors and rainflow counting have sufficient accuracy for tracking and cycle counting of hours-long continuous arm motion? If so, what are the cycle rates of normal arm ADL and is there a representative cycle that can serve as a 'gait cycle' for the arm?

Methods: IMU sensors continuously tracked a robot performing 8 h of simulated cyclic arm motion. Error in the angle measurements was regressed against time to determine the rate of error and the total accumulated error. Additionally, the cycle count accuracy of rainflow, peak/valley, and Fourier transform counting methods was evaluated.

Results: Over 8 h the IMU measurements accumulated a maximum 0.473° of error and the rainflow method counted cycles with less than 1% error. Applying rainflow counting to normal shoulder ADL resulted in an average rate of 533 elevation cycles per day.Tabulating the ADL cycles by mean and range values into a matrix and calculating the centroid, the single best values representing arm elevation cycles were a mean of 22.4° and a range of 21.6°.

Significance: IMU sensors can track arm motion for 8 h with little increase in error, though during longer durations error may reach unacceptable levels. For normal arm ADL, the rainflow determined count of arm elevation full-cycles differed from previous estimates based on peak/valley counting. From the rainflow counting, a single cycle representation of cycle mean and range was determined that can be used as a 'gait cycle' for the shoulder

1. Introduction

Inertial Measurement Units (IMUs) are convenient for joint motion tracking outside of laboratory settings because of their low cost and ease of use. Reports have established the accuracy of IMU sensors when capture durations are seconds to minutes long [1], but longer times may be needed for occupational, recreational, and therapeutic applications [2–6]. However, IMU sensors may be influenced by drift of the gyroscopes and electromagnetic interference [1,3,7,8] and there is little evidence demonstrating how error may accumulate during hours-long, continuous use. Obtaining accurate hours-long IMU based motion tracking would also be useful for establishing cycle counts of upper arm motion during activities of daily living (ADL).

Cycle counts are used to benchmark orthopedic implant fatigue testing, patient activity levels, and in assessing workplace related injuries [2–4,9,10], but there is a scarcity of reports addressing arm cycle counting methods and their accuracy. For hip/knee joints, gait is recognized as the most frequently performed activity [11] and the predominantly planar motion of hip/knee joints simplifies cycle identification and counting. Because of this simplicity, pedometers have been sufficient for cycle counting [12].

For the upper arm, cycle identification and counting has been hampered the lack of a recognized dominate activity [11]. Further, unlike hip/knee gait motion which consists of a series of organized, repeated cycles, upper arm motion during unrestricted ADL (containing multiple activities) may not organize into a series of repeating cycles.

E-mail address: Bryan.Kirking@enovis.com.

https://doi.org/10.1016/j.gaitpost.2022.11.020
Received 8 July 2022; Received in revised form 26 October 2022; Accepted 29 November 2022
Available online 1 December 2022

Because of these challenges, and the relative newness of IMU sensors, there are few studies describing cycle counting of three dimensional arm motion during unrestricted ADL.

When a specific task or activity is being monitored, such as during repetitive workplace tasks, cycle counting algorithms may be trained to recognize a target cycle [13]. More generalizable frequency-based methods that use a representative frequency [4,6] have also been described. However, due to the irregularity of ADL motion, methods that make fewer assumptions about the signal may demonstrate better performance.

ASTM E1049 ‘Cycle Counting in Fatigue Analysis’ describes a “compilation of acceptable procedures for cycle-counting methods” and has been applied to structures where loading often appears random. It is hypothesized that due to the unorganized appearance of upper arm motion, the rainflow counting method from E1049 would be well suited to cycle counting.

The aims of this study were to demonstrate the error accumulation during hours-long, continuous IMU monitoring of joint motion, verify the cycle counting accuracy of methods when applied to IMU cyclic motion data, and finally demonstrate rainflow cycle counting on previously collected hours-long ADL of the upper arm.

2. Methods

2.1. Robot setup

A Fanuc M-201A robot was programmed to simulate idealized upper arm cycles. A robot was used rather than humans to obtain controlled, consistent, and repeatable motion cycles over a continuous 8-hour duration representing a typical work shift. Additionally, the use of the robot allowed rigid mounting of the IMU to isolate sensor error and avoid confounding effects from soft tissue. The idealized motions were flexion-extension (FE) from − 30–60° (0° with arm at side), adduction-abduction (AA) from − 15–60° (0° with arm at side), and internal-external (IE) from − 80–30° (0° aligned with frontal plane normal, internal rotation negative) motions (Fig. 1-top) performed at a constant angular velocity and representing typical joint angles expected during ADL [6,10,14,15] The robot performed serial motion of each FE/AA/IE four times and then the robot torso and arm segments were simultaneously rotated 20° in the horizontal plane. The FE/AA/IE motions were then repeated at a higher velocity as shown in Fig. 1-bottom for a total of four velocities (7.5, 15, 30, and 60°/sec) representing the bandwidth of human speeds [8]. After the fastest velocity, the robot torso and arm were simultaneously rotated in the horizontal plane, back to the starting position and the entire sequence was repeated continuously for 8 h resulting in 712 cycles each of FE, AA, and IE.

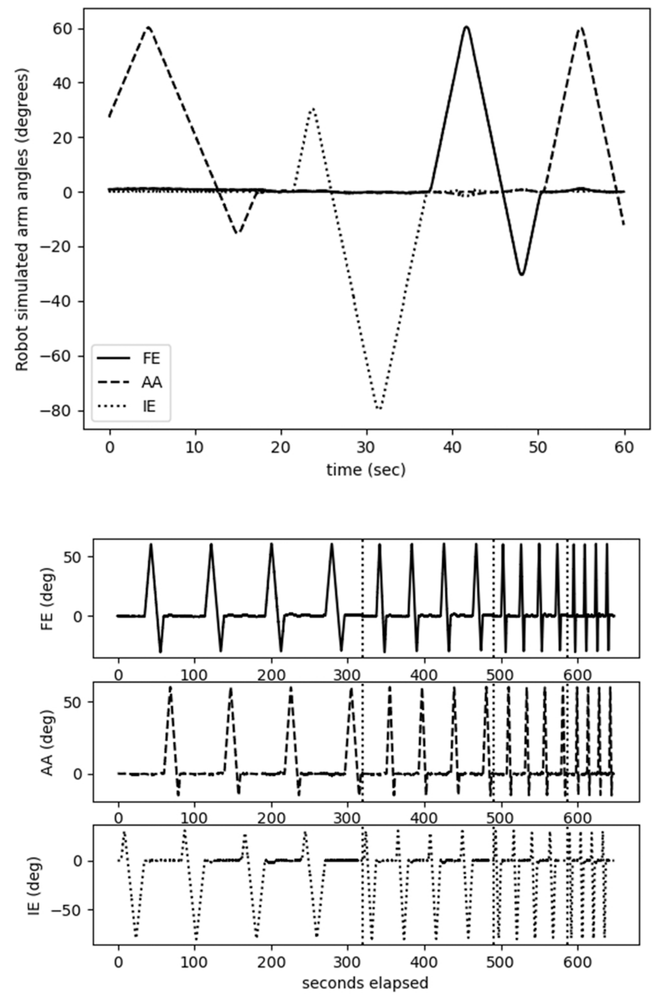

Fig. 1. Top- Relative timing of flexion-extension (solid), adduction-abduction (dashed), and internal-external (dotted) simulated arm rotations. Bottom- Full sequence of simulated arm motions. Vertical lines indicate where speed changed.

2.2. IMU sensors and optotrak

The IMU sensor data was used to calculate three dimensional arm angles using an Unscented Kalman filter [6]. To match the sensor configurations described in [6], one APDM Opal v1 IMU sensor was rigidly attached to the robot in a vertical position corresponding to a human torso sensor placed on the manubrium. A second Opal v1 sensor was rigidly attached to another segment that had 3 rotational degrees of freedom from the trunk sensor and in a position corresponding to the lateral aspect and aligned with the long axis of a human arm. The initial orientation of the sensors was recorded and usde to establish the neutral position. An Optotrak Certus video tracking system with 4 active marker flags attached on the arm segment of the robot captured the first full sequence of motion (4 FE/AA/IE motions at 4 velocities) at the start of each hour to use as the ground truth. As the Optotrak measurements could not be recorded continuously, the 8 Optotrak files from each hour were coarse synchronized to the corresponding section of the IMU data using the file save times and then further refined by manually aligning the data point of the first flexion/extension peak from each Optotrak file to the corresponding IMU flexion/extension peak data point. This optimized comparing the angle estimates but removed timing/synchronization differences between the systems which was beyond the intended scope.

2.3. Temporal error analysis of the IMU data of robot motion

For each hour, the IMU determined angles were resampled from 128 Hz to the Optotrak frequency of 100 Hz and the averaged absolute error (AAE) was calculated. The AAE average was then plotted by hour and a linear fit of AAE and elapsed time was used to estimate the rate of accumulated AAE and the total accumulated AAE over the 8 h collection time.

2.4. Verification of cycle counting methods

Three counting methods were performed to evaluate their accuracy for counting arm cycles. The counting methods were a Fourier transform with median power frequency (MPF), peak/valley, and rainflow. FFT/MPF counting was done using Python library FFT functions, calculating the MPF, and then multiplying the MPF by the trial duration [6]. The rainflow counting and peak/valley counting were performed using the python module fatpack (Gunnstein Thomas Frøseth). Note that rainflow counting identifies half cycles and then matches to a similar, opposite half cycle to produce full cycle counts, unlike peak/valley which only provides half cycles counts.

Counting methods were conducted on four test signals with known cycle counts: a sine wave at 0.1 Hz, the initial 16 robot arm FE cycles measured with the Optotrak, the initial 16 robot arm FE cycles measured from IMUs, and the full 8-hour robot FE data measured from IMUs.

Before counting, signals were low pass filtered at 8hz with a Butterworth filter to remove frequencies higher than expected human movement [8]. During peak/valley counting, a 10° threshold was used to eliminate 'non-deliberate' motions as described by Langohr [10]. To be consistent, rainflow counts were racetrack filtered at 10° before counting. The rainflow bin size was set to 4 degrees (90 bins over +/−180°). The cycle rate was then estimated by dividing the number of rainflow counted cycles by the total trial duration.

2.5. Application of cycle counting to arm motion from previous data

Using previously reported data of normal subjects performing unrestricted work and recreational ADL [6], the rainflow cycle counts, peak/valley counts, and cycle rate were determined for each subject and trial. An output of the rainflow counting method is a matrix that tabulates the number of cycles for each mean and range combination. For the ADL data, the centroid of the rainflow matrix for each subject and trial was calculated by multiplying the mean and range values by the squared number of observations and dividing by the total number of observations squared.

3. Results

3.1. Temporal error analysis of the IMU data of robot motion

The FE, AA, and IE motions from the first hour of cycles is shown in Fig. 2. In Fig. 2A, all three IMU angles are shown together to demonstrate the sequence of rotations. In Fig. 2B to Fig. 2D, the IMU angles are shown as a solid line with the corresponding Optotrak angles shown as a dashed line to demonstrate the relative accuracy of the IMU.

For all angles, the shape of the IMU angle was well matched to the Optotrak. IMU IE showed the most error relative to the Optotrak IE with the largest difference occurring primarily in the neutral / zero velocity portion of the IE curve.

Fig. 3 shows the AAE plotted by hour to demonstrate the error accumulation in each hour. Additionally, the associated linear regression line for each motion plane is plotted to demonstrate the overall error accumulation rate. The regression indicated that the rate of AAE by hour was 0.016°/hr for FE, 0.009°/hr for AA, and 0.059°/hr for IE. At these error rates, the total increase in AAE over 8 h for FE, AA, and IE was 0.130°, 0.071°, and 0.473° respectively. The associated percent increase in AAE over 8 h from the initial period was 17.6 % for FE, 6.8 % for AA, and 11.3 % for IE.

3.2. Verification of cycle counting methods

The number of counts from each method on the test signals is shown in Table 1. For the sine wave with 6 full cycles (12 half cycles), both the FFT/MPF and rainflow methods produced the correct full cycle count. The peak/valley counted 13 half cycles. Note that the peak/valley counts are half cycles rather than full cycles.

For the Optotrak/robot trial, rainflow produced the actual full cycle

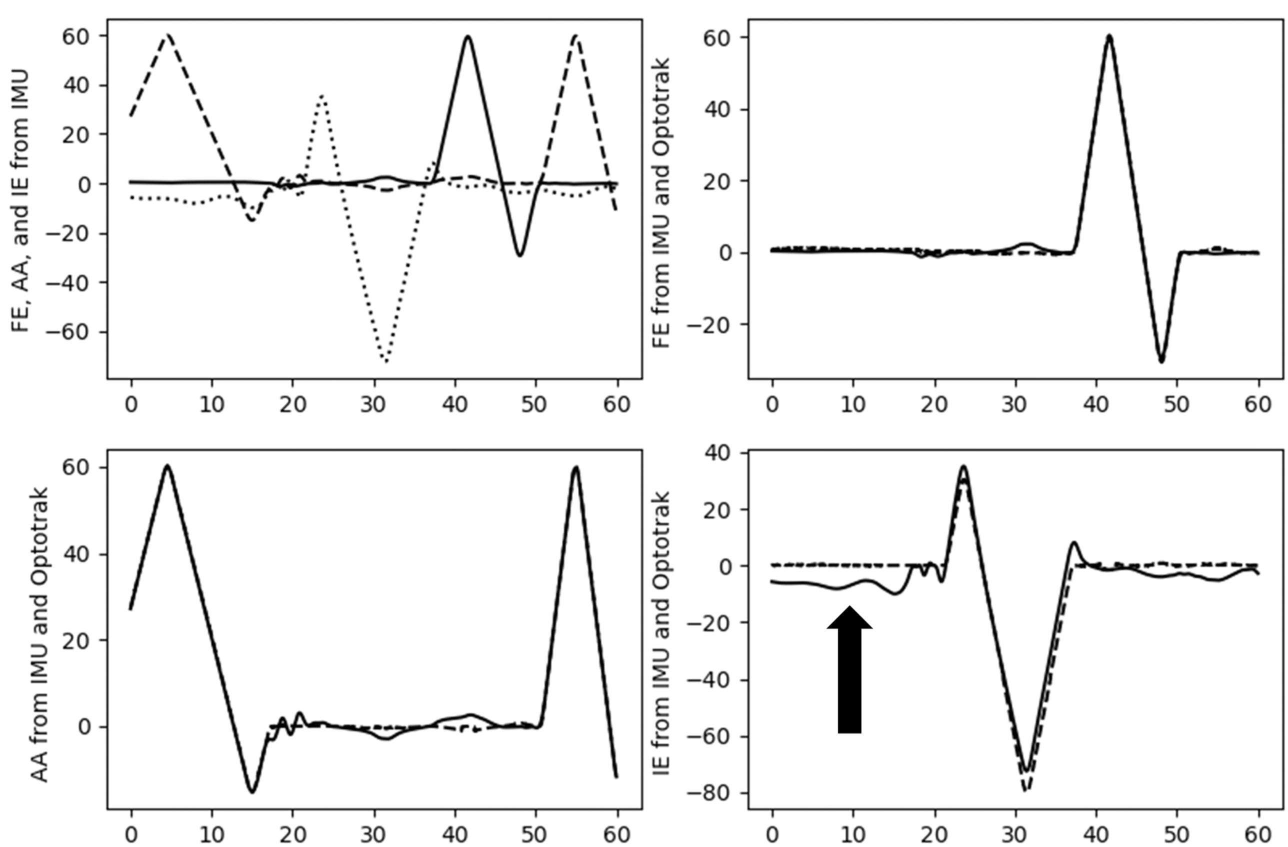

Fig. 2. A) [Top,left]: Flexion-extension (solid), abduction-adduction (dashed), and internal-external (dotted) motions measured from the IMU data. Superimposed IMU (solid) and Optotrak (dashed) motions in Flexion-extension B)[Top,right], abduction-adduction C)[Bottom,left], and internal-external rotation D)[Bottom, right]. Arrow points to the largest error which occurred during the still portion of IE rotation.

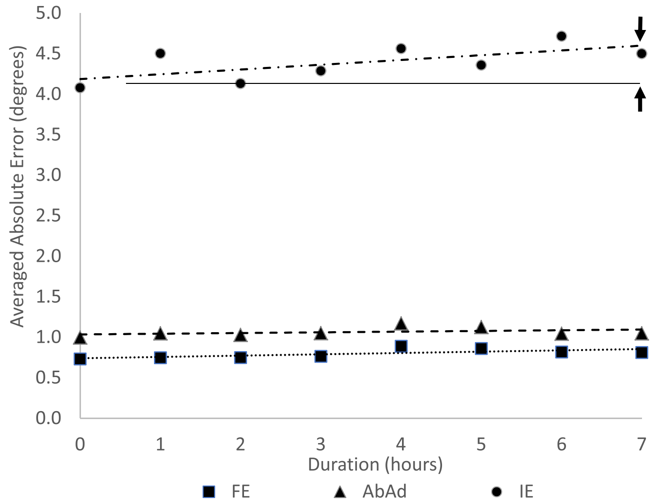

Fig. 3. Averaged absolute error in angle estimates during each hour. Arrows indicates the accumulated AAE in internal-external rotation after 8 h of continuous collection.

Table 1
Cycle counts produced by the three counting methods on four test signals.

	Actual Cycles	FFT/ MPF	Peak/ Valley	Rainflow
Sine wave, 0.1 Hz	6	6	13	6
Robot-Optotrak cycles 1–16 of F/E	16	50	39	16
Robot-IMU cycles 1–16 of F/E	16	64	49	16
Robot IMU cycles 1–712 of F/E (8 hrs)	712	2648	2155	718

count of 16. The peak/valley method produced 39 half cycles which was seven half cycles greater than the expected 33 half cycles. The FFT/MPF method produced 50 full cycles which was 34 more than actual.

For the IMU/robot trial, rainflow produced the actual full cycle count of 16. The peak/valley method produced 49 half cycles which was 17 half cycles greater than the expected 32 half cycles. The FFT/MPF method produced 50 full cycles which was 34 more than actual. When counting the complete 8-hour trial with 712 full cycles, rainflow counted 718 full cycles (<1 % error), peak/valley counted 2155 half cycles (730 greater than the expected 1425 half cycles, 51 % error) and FFT/MPF counted 2648 full cycles (1936 greater than actual, 272 % error).

3.3. Application of cycle counting to arm motion from previous data

The rainflow cycle counting and peak/valley counting methods of the IMU data from ADLs is presented in Table 2. Cycle counts of arm angles ranged from 450 to 1118 full cycles per hour (fcph) from the rainflow method and half cycles ranged from 1071 to 3266 half cycles per hour (hcph) using peak/valley. The centroid of the rainflow matrix for each arm angle produced cycle means/ranges of: elevation 22.4° / 21.6°, elevation plane heading 87.1° / 40.2°, FE 3.8° / 22.0°, AA − 2.9° / 22.0°, and IE − 13.1° / 25.1°.

4. Discussion

4.1. Temporal error of IMU tracked robot motion

IMU predicted arm angles tracked well against the Optotrak measured angles with AAE on the order of 1° or less and IE AAE of about 4°. These baseline errors were in the reported ranges for IMU measurements of shoulder kinematics [16,17]. FE demonstrated an

Table 2
Cycle rates of normal shoulder ADL and the centroid of the Rainflow matrix. Cycle rates are per hour.

Motion Axis		Rainflow full cycle rate	Peak/Valley half-cycle rate	Mean	Range
		fcph	hcph	deg	deg
Upper arm elevation	mean	533	1183	22.4	21.6
	std	180	401	5.1	2.4
Angle of the arm elevation plane	mean	1118	3266	87.1	40.2
	std	362	1047	6.3	10.4
Flexion/Extension	mean	450	1080	3.8	22.0
	std	136	339	7.8	2.8
Abduction/ Adduction	mean	478	1071	-2.9	22.0
	std	179	396	9.3	5.3
Internal/External	mean	617	1440	-13.1	25.1
	std	201	488	9.8	2.7

accumulated error of 0.13°, which combined with the smallest time zero error of 0.74° created the largest percentage error of 17.6°. IE had the largest AAE accumulation of 0.47° (11.3 %) as was expected because the pure horizontal plane rotations of the arm and torso segments represent a challenge condition due to the lack of a consistent reference for heading. These data demonstrated that when using an Unscented Kalman filter algorithm to estimate arm joint angles from IMU sensors, error accumulation did occur over an 8 h duration and exceeded 10 % of the time zero AAE. It should be noted that the IMUs were firmly attached to the robot segments and would not include errors due to IMU motion relative to the underlying joint segments such as slipping of the sensors, or errors due to differences in skin/bone motion. Further, the range of studied angles did not include angles near the extreme range of motion which are infrequent but could lead to issues such as gimble lock.

4.2. Verification of cycle counting methods

Across all validation trials, rainflow counting produced the most accurate cycles counts, with less than 1% error in the full 8-hour IMU/ robot trial.

The peak/valley counting method was tested to recreate the counts described in Langhor [10]. While both peak/valley and rainflow begin by counting single directional motions from reversals, rainflow takes an additional step to match the directional motions to form full cycles. Because peak/valley counting does not pair into full cycles, peak/valley was expected to over count full cycle counts by about 2:1. Peak/valley counting performed well for the sine wave trial but count error increased to 22% on the robot/Optotrak trial and reached 51% on the full 8-hour robot/IMU trial, even when accounting for the difference in half-cycles / full-cycles.

The FFT/MPF had the largest errors of the counting methods. The error in the FFT/MPF may partially result from the FFT fitting high frequency components in order to reproduce the triangular wave form of the robot motion. Further, trying to represent a complex power spectra like the ADLs where the underlying signal is not necessarily periodic with a single representative frequency maybe insufficient. More complex frequency domain techniques [18,19] may be better suited for analyzing arm cycles of ADL.

4.3. Application of cycle counting to arm motion from previous data

Using the peak/valley counting method on ADL elevation of normal arms tracked with IMUs resulted in a cycle rate of 1183 half-cycles/hr. Langohr [10] reported half-cycle counts of 820 half-cycles/hr in post operative arthroplasty shoulders that were at least 1 year post implantation and 842 half-cycles/hr in the contralateral, unoperated shoulder. The larger count for the normal shoulders is likely due to a difference in age-related activity levels of the two study populations.

Using the FFT/MPF method, a 10 year cycle value of 649,009 cycles was previously calculated [6] for the same IMU-ADL data set reanalyzed in this study. Given the poor performance demonstrated by the FFT/MPF method on the validation signals, that previous estimate is likely inaccurate compared to the rainflow counted cycles.

Using the rainflow average elevation cycle rate and assuming 8 h of work and 8 h of recreation each day extrapolates to an estimated 28 million elevation full-cycles for a 10-year period. 2740 cycles per day (10 million cycles per 10 years) is often used in testing lifetime performance of hip and knee devices, though a recent review reported that healthy adults over 20 years of age perform closer to 7000 cycles per day (25.5 million per 10 years). The rainflow based count of the arm ADL data of 450 flexion/extension cycles per hour equates to 7206 cycles per day (26.3 million per 10 years). As people tend to swing their arms in flexion/extension during gait [20], the number of non-gait related, 'deliberate' (> 10 degrees) flexion-extension arm cycles appears to be in the range of 206 cycles/day to 4466 cycles/day.

4.4. Representing a typical arm motion cycle

An example of the rainflow matrix of the observed cycles from the normal ADL IMU motion is shown in Fig. 4. The example demonstrates that the matrix cells with the largest counts were clustered near a cycle mean of 18° and cycle range of 14°. Cycle counts then reduced and spread out with increasing cycle mean and range. This distribution is similar to the report by Langhor [10] who noted the largest amount of time was spent with the arm between 20°– 40° of elevation with decreasing amounts of time spent at angles above 40°.

To determine a single value of cycle mean and cycle range that represented the full matrix of cycles, the centroid of the matrix observations was calculated by weighting the mean and range by the square of the observations. Two other approaches that were explored included using the matrix cell with the largest number of observations and taking the weighted average of the mean and range observations. The cell with the most observations was discarded because it was inconsistently located among the trials. The weighted average was discarded because it appeared to be overly influenced by cells that had large cycle mean or cycle range values but a corresponding small number of observations.

Across all ADL trials, the average of the centroids from each rainflow matrix of arm elevation resulted in a cycle mean of 22.4° and a cycle range 21.6°. Note that because elevation is always positive, the mean of the elevation cycle was not centered near 0° as it was for flexion–extension and abduction–adduction. The plane of the elevation had a cycle mean and range of 87.1° and 40.2° and the internal-external rotation of the humerus had a cycle mean and range of – 13.1° (internally rotated) and 25.1°. These cycle mean and range values represent the most typical motion of normal shoulders and could be used as a 'gait cycle' of the upper arm when evaluating shoulder function or for conducting lifetime testing and simulations of treatments and devices such as total joint replacements.

5. Conclusion

Using a robot to simulate arm motion for eight continuous hours, IMU based angle measurements demonstrated a maximum accumulated average absolute error of 0.473°, but longer duration tasks could develop unacceptably large error. Using the same robot simulated motion, rainflow cycle counting demonstrated an error of less than 1%. Applying rainflow counting to previously collected IMU data on the ADLs of normal shoulders produced 533 full cycles of arm elevation per hour. Finally, rainflow counting on IMU collected arm ADL motion was used to determine a cycle mean and range value which can be used as a 'gait cycle' for the shoulder. For arm elevation, the cycle mean was 22.4° and the cycle range was 21.6°.

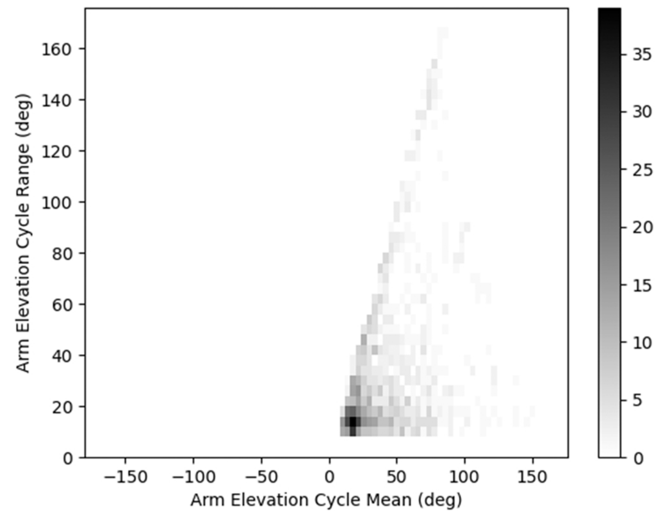

Fig. 4. An example of the observed counts for cycle mean / cycle range combinations produced by the rainflow method during unrestricted/free ADL. Gray scale represents the number of observations of each cycle mean and range combination.

Funding

This work was funded by Enovis.

Conflict of interest

The author is an employee of Enovis.

Acknowledgement

The author would like to acknowledge the efforts of Nathan Pyle from Enovis who translated the IMU tracker code from MATLAB to python and assisted with editing the manuscript. Additionally, the efforts of Heath Henninger from the University of Utah who setup the robot and Optotrak systems and assisted with the rigid body conversions.

References

[1] I. Weygers, M. Kok, M. Konings, H. Hallez, H. De Vroey, K. Claeys, Inertial sensor-based lower limb joint kinematics: a methodological systematic review, Sensors 20 (2020) 673, https://doi.org/10.3390/s20030673.
[2] B. Coley, B.M. Jolles, A. Farron, K. Aminian, Arm position during daily activity, Gait Posture 28 (2008) 581–587, https://doi.org/10.1016/j.gaitpost.2008.04.014.
[3] S. Lim, C. D'Souza, A narrative review on contemporary and emerging uses of inertial sensing in occupational ergonomics, Int. J. Ind. Ergon. 76 (2020), 102937, https://doi.org/10.1016/j.ergon.2020.102937.
[4] D. Álvarez, J.C. Alvarez, R.C. González, A.M. López, Upper limb joint angle measurement in occupational health, Comput. Methods Biomech. Biomed. Eng. 19 (2016) 159–170, https://doi.org/10.1080/10255842.2014.997718.
[5] B. Pedro, F. João, J.P.R. Lara, S. Cabral, J. Carvalho, A.P. Veloso, Evaluation of upper limb joint contribution to racket head speed in elite tennis players using imu sensors: comparison between the cross-court and inside-out attacking forehand drive, Sensors 22 (2022) 1283, https://doi.org/10.3390/s22031283.
[6] B. Kirking, M. El-Gohary, Y. Kwon, The feasibility of shoulder motion tracking during activities of daily living using inertial measurement units, Gait Posture 49 (2016) 47–53, https://doi.org/10.1016/j.gaitpost.2016.06.008.
[7] X. Robert-Lachaine, H. Mecheri, C. Larue, A. Plamondon, Validation of inertial measurement units with an optoelectronic system for whole-body motion analysis, Med Biol. Eng. Comput. 55 (2017) 609–619, https://doi.org/10.1007/s11517-016-1537-2.
[8] L. Ricci, F. Taffoni, D. Formica, On the orientation error of IMU: investigating static and dynamic accuracy targeting human motion, PLoS One 11 (2016), e0161940, https://doi.org/10.1371/journal.pone.0161940.
[9] F04 Committee, Specification for Shoulder Prostheses, ASTM International, n.d. ⟨https://doi.org/10.1520/F1378–18E01⟩.
[10] G.D.G. Langohr, J.P. Haverstock, J.A. Johnson, G.S. Athwal, Comparing daily shoulder motion and frequency after anatomic and reverse shoulder arthroplasty,

J. Shoulder Elb. Surg. 27 (2018) 325–332, https://doi.org/10.1016/j.jse.2017.09.023.
[11] C.J. van Andel, N. Wolterbeek, C.A.M. Doorenbosch, D.H.E.J. Veeger, J. Harlaar, Complete 3D kinematics of upper extremity functional tasks, Gait Posture 27 (2008) 120–127, https://doi.org/10.1016/j.gaitpost.2007.03.002.
[12] C. Tudor-Locke, C.L. Craig, W.J. Brown, S.A. Clemes, K. De Cocker, B. Giles-Corti, Y. Hatano, S. Inoue, S.M. Matsudo, N. Mutrie, J.-M. Oppert, D.A. Rowe, M. D. Schmidt, G.M. Schofield, J.C. Spence, P.J. Teixeira, M.A. Tully, S.N. Blair, How many steps/day are enough? for adults, Int. J. Behav. Nutr. Phys. Act. 8 (2011) 79, https://doi.org/10.1186/1479-5868-8-79.
[13] O. Akkas, C.-H. Lee, Y.H. Hu, T.Y. Yen, R.G. Radwin, Measuring elemental time and duty cycle using automated video processing, Ergonomics 59 (2016) 1514–1525, https://doi.org/10.1080/00140139.2016.1146347.
[14] D.J. Magermans, E.K.J. Chadwick, H.E.J. Veeger, F.C.T. van der Helm, Requirements for upper extremity motions during activities of daily living, Clin. Biomech. 20 (2005) 591–599, https://doi.org/10.1016/j.clinbiomech.2005.02.006.
[15] M.W. Maier, M. Niklasch, T. Dreher, F. Zeifang, O. Rettig, M.C. Klotz, S.I. Wolf, P. Kasten, Motion patterns in activities of daily living: 3- year longitudinal follow-up after total shoulder arthroplasty using an optical 3D motion analysis system, BMC Musculoskelet. Disord. 15 (2014) 244, https://doi.org/10.1186/1471-2474-15-244.
[16] A. Carnevale, U.G. Longo, E. Schena, C. Massaroni, D. Lo Presti, A. Berton, V. Candela, V. Denaro, Wearable systems for shoulder kinematics assessment: a systematic review, BMC Musculoskelet. Disord. 20 (2019) 546, https://doi.org/10.1186/s12891-019-2930-4.
[17] K. Lebel, P. Boissy, M. Hamel, C. Duval, Inertial measures of motion for clinical biomechanics: comparative assessment of accuracy under controlled conditions – changes in accuracy over time, PLoS One 10 (2015), e0118361, https://doi.org/10.1371/journal.pone.0118361.
[18] Q. Meng, B. Li, H. Holstein, Recognition of human periodic movements from unstructured information using a motion-based frequency domain approach, Image Vis. Comput. 24 (2006) 795–809, https://doi.org/10.1016/j.imavis.2006.01.033.
[19] A. Godfrey, R. Conway, D. Meagher, G. ÓLaighin, Direct measurement of human movement by accelerometry, Med. Eng. Phys. 30 (2008) 1364–1386, https://doi.org/10.1016/j.medengphy.2008.09.005.
[20] S.H. Collins, P.G. Adamczyk, A.D. Kuo, Dynamic arm swinging in human walking, Proc. R. Soc. B 276 (2009) 3679–3688, https://doi.org/10.1098/rspb.2009.0664.